Korean J. Chem. Eng., **22**(2), 219-227 (2005)

Studies on the Modeling Calculations of the Unit Molten Carbonate Fuel Cell

Ye-Ro Lee, Min-Jung Yoo, Gui-Yung Chung†, Hee-Chun Lim*, Tae-Hoon Lim, Suk-Woo Nam** and Seong-Ahn Hong****

Department. of Chemical Engineering, Hong-Ik University, 72-1 Sangsudong, Mapoku, Seoul 121-791, South Korea
*Korea Electric Power Research Institute (KEPRI), 103-16 Munjidong, Yuseonggu, Daejon 305-380, South Korea
**Battery & Fuel Cell Research Center, Korea Institute of Science and Technology (KIST),
P.O. Box 131 Cheongryang, Seoul 130-650, South Korea
(*Received 26 October 2004 • accepted 23 December 2004*)

Abstract–One parameter should be fixed in the process of simulating the performance of a unit MCFC (molten carbonate fuel cell). Distributions of temperature, conversions of hydrogen, and cell performance have been obtained in two different methods: one with a fixed value of cell voltage and the other with a fixed value of current density. Results by both methods have been compared with experimental data. The method with the fixed value of cell voltage resulted in a more reasonable fitting to experimental data.

Key words: MCFC, Analytical Methods, Cell Performances, Simulation

INTRODUCTION

Molten carbonate fuel cell (MCFC) has a high efficiency and a low emission of NO_x and SO_x and it can be established in a smaller space. The MCFC operates at a high temperature, about 650 °C, so it is able to accelerate the electrochemical reaction without Pt catalyst [Appleby and Foulkes, 1989]. Furthermore, one of many advantages of MCFC is that the water-gas shift reaction consuming CO is occurring in the MCFC. With these advantages, MCFC is generally considered as a second-generation fuel cell.

Many parameters are related to each other in operating and estimating the MCFC. For example, mass and heat transfer, chemical reaction, and electrical correlation are used to estimate the operation of MCFC. For this reason, many numerical analysis methods of MCFC have been studied. Sampath and Sammels [1980] developed a numerical analysis model for obtaining distributions of current density in an isothermal unit fuel cell. Wolf and Wilemski [1983] have studied temperature distributions in a single cell by applying a simplified model of cell performance. Cao and Masubuchi [1991] obtained the dynamic characteristics of temperature in a unit cell. Kobayashi et al. [1988] and Fujimura et al. [1991] have calculated temperature distributions of single cells and stack by applying mass transfers to the chemical reactions occurring in the fuel cell and applied a thin-film cylindrical-pore model to study the relation between current density and cell voltage. Koh et al. [2000] have made a stack mode, predicted the temperature distribution at a constant-load operation, and compared with measured data for a 5 kW stack.

In our previous research, the mathematical analysis for the MCFC 100 cm^2 unit cell, including the effect of water-gas shift reaction, at a constant current density (i) was studied [Kim et al., 2002]. In the actual MCFC, as anode and cathode gases react keenly, current density changes greatly, so it is necessary to study distributions of current density. Therefore, most mathematical analysis models have been developed at a constant cell voltage, i.e., assuming a constant voltage all through the cell [Kim et al., 1995; Ahn et al., 1994; Park et al., 2002; Lee et al., 2004]. Likewise, it is mathematically possible to develop the analysis model either at a constant current density or at a constant cell voltage.

Considering this point, distributions of temperature, compositions of oxidant and fuel gases, and performances of a single cell are examined both at a constant cell voltage and at a constant current density in this research. For convenience, the calculations made at a constant cell voltage are named as method A and those made at a constant current density as method B. Both results by methods A and B have been compared with each other and also with experimental data. We have tried to supply basic reasoning for selecting a calculation method by describing how the calculation results by the two methods are different from each other.

MATHEMATICAL MODELING

1. System of MCFC

Reactions involved in MCFC are the reduction of oxidant gas in a cathode electrode and the oxidation of fuel gas in an anode electrode. The oxidant gas is supplied to the cathode and forms carbonate ions as in Eq. (1). These ions are transported perpendicularly toward the anode. In the anode reaction, water and carbon dioxide are formed as in Eq. (2).

$$\text{(cathode)} \quad CO_2 + \frac{1}{2}O_2 + 2e^- \rightarrow CO_3^{2-} \tag{1}$$

$$\text{(anode)} \quad H_2 + CO_3^{2-} \rightarrow CO_2 + H_2O + 2e^- \tag{2}$$

A significant advantage of a high-temperature fuel cell such as MCFC is its ability to utilize CO as a fuel. The water-gas shift reaction in Eq. (3) reaches equilibrium rapidly at 650 °C to produce H_2.

$$CO + H_2O \leftrightarrow CO_2 + H_2 \tag{3}$$

As H_2 is consumed in the anodic reaction of Eq. (2), the reaction is driven to the right to reach an equilibrium state by Eq. (3). Both H_2O and CO_2 are produced in an equal amount. Because of the shift

†To whom correspondence should be addressed.
E-mail: gychung@hongik.ac.kr

reaction, the utilization of fuel in MCFC can exceed the utilization of H_2, based on the inlet concentration of H_2. The better utilization of fuel is possible because the shift reaction provides the additional fuel, H_2, in the anode gas [Appleby and Foulkes, 1989].

Since the water-gas shift reaction is rapid in the presence of metals such as nickel, the following equilibrium relationship for this reaction is easily obtained [Smith and van Ness, 1987; Ahn et al., 1995].

$$K_s = \frac{(p_{H_2})(p_{CO_2})}{(p_{H_2O})(p_{CO})} = \frac{(X_h)(X_{ca})}{(X_w)(X_{co})} \tag{4}$$

$$K_s = 157.02 - 0.4447T + 4.2777\times10^{-4} - 1.3871\times10^{-7}T^3 \quad (\approx 2 \text{ at } 650\,^{\circ}\text{C}) \tag{5}$$

Here, T [K] is the temperature of the cell.

Fig. 1(a) and (b) show the operating principles and a schematic diagram of the MCFC. The anode gas (fuel gas) flows in the *x*-direction and the cathode gas (oxidant gas) flows in the *y*-direction. The gas channels are ignored and the cross-sections of the gas flows are assumed to be rectangular. The compositions of gases are assumed to be uniform through the z-direction.

The heat generated by the electrochemical reaction is transferred to the anode and cathode gases, separate plates, and electrode-electrolyte plate by convection and radiation. Heat and mass transfers in the z-direction are ignored because the thicknesses of the separate plate, the gas channel and the electrode-electrolyte are very thin compared to the width and the length of a single cell. The radiation energy absorbed by anode and cathode gases is ignored.

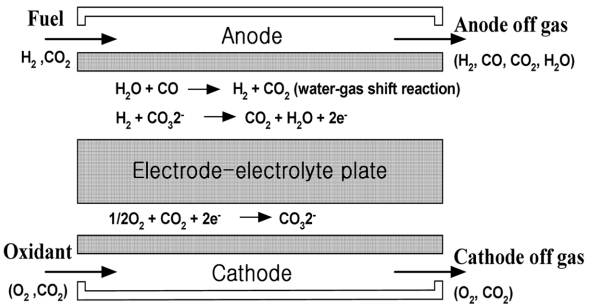

(a) Operating principles

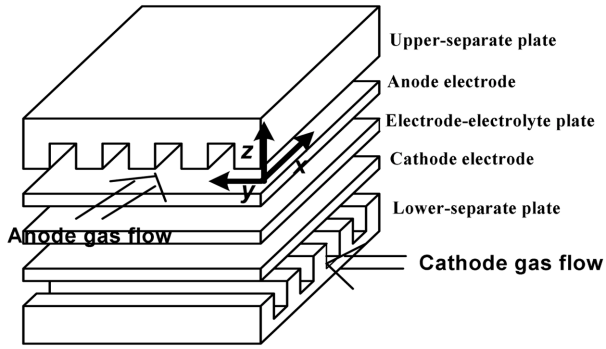

(b) Schematic diagram (the cross flow type)

Fig. 1. The operating principles and the schematic diagram of an MCFC.

2. Governing Equations

2-1. Mass Balance

The mass balances of anode and cathode gases are as follows:

For the anode gas;

$$\frac{1}{W}\frac{\partial(n_a X_k)}{\partial x} + \nu_{E,k}\frac{i}{2F} + \nu_{S,k}\frac{G_s}{\Delta x \Delta y} = 0 \tag{6}$$

Here, n_a is the mole flow rate of anode gas [mol/hr], X_k the composition of k-component in the anode gas, W the width of the cell [m], and F the Faraday's constant, 26.8 A·hr/mol. $\nu_{E,k}$ and $\nu_{S,k}$ are the stoichiometric coefficients of the k-component in the electrochemical reaction and the water-gas shift reaction, respectively. G_S [mol/hr] is the molar rate of generation or consumption of hydrogen by the water-gas shift reaction in the volume of ($\Delta x \Delta y b_g$). n_a [mol/hr] denotes the total anode gas flow rate including hydrogen and carbon monoxide. For the calculation of n_a, the hydrogen flow rate, n_{H_2}, is calculated first by using the utilization of hydrogen, u_H, and the total current density, i.

For the cathode gas, the water-gas shift reaction is not included.

$$\frac{1}{L}\frac{\partial(n_c X_k)}{\partial y} + \nu_{E,k}\frac{i}{F} = 0 \tag{7}$$

The equilibrium relationship for the water-gas shift reaction is easily obtained as in Eq. (4) with partial pressures and compositions of each gas [Smith and van Ness, 1987; Ahn et al., 1995].

2-2. Energy Balance

The same equations of energy balance studied previously are used [Kim et al., 1999; Leo et al., 1992].

For the upper separator;

$$\frac{\partial^2 T_s}{\partial x^2} + \frac{\partial^2 T_s}{\partial y^2} = \frac{h_{res}}{b_s k_s}(T_s - T_e) + \frac{h_{sga}}{b_s k_s}(T_s - T_{ga}) + \frac{h_{sb}}{b_s k_s}(T_s - T_b) \tag{8}$$

b.c. 1.: at x=0 and x=L, all y; $\frac{\partial T_s}{\partial x} = 0$

b.c. 2.: at all x, y=0 and y=W; $\frac{\partial T_s}{\partial y} = 0$

Here, the left-hand terms are heat transfer by conduction and the right-hand terms are the radiation heat transfer between the separator and the electrode-electrolyte plate, the convectional heat transfer between the separator and the anode gas, and the convectional heat transfer between the separator and the surrounding of the cell, respectively. The heat transfer coefficients, h's, were decided by calculating Nusselt number [McCabe et al., 2001]. A similar equation can be written for the lower separator.

The heat of the water gas shift reaction (q_S) is included in the following energy balance equation for the anode gas.

For the anode gas;

$$\frac{\partial}{\partial x}(m_a C_{pa} T_{ga}) = h_{ega}(T_e - T_{ga}) + h_{sga}(T_s - T_{ga}) + \sum_k G_{ai} C_{pa,k} b_g T_{ga} + q_S \tag{9}$$

b.c.: at x=0, all y; $T_{ga} = T_i$

Here, the left-hand term represents the enthalpy change of gas. The first two terms on the right-hand are convectional energy transfers. The third term is the enthalpy change of each component generated or consumed by the reaction. The last term is the heat of shift

reaction. The equation for the cathode gas can be written similarly as Eq. (9) without q_S. The heat of reaction for the shift reaction, q_S [J/hr] in Eq. (9), is as follows.

$$q_S=\Delta H_S\cdot\Delta G_{CO} \tag{10}$$

Here, ΔG_{CO} [mol/hr] is the consumption rate of CO by the shift reaction and ΔH_S [J/mol], the enthalpy change of the shift reaction, is calculated as a function of temperature [Smith and van Ness, 1987].

$$\Delta H_S=-9{,}932.5-0.515T+(3.117\times10^{-3})T^2-(1.05\times10^{-6})T^3 \tag{11}$$

For the electrode-electrolyte plate:

$$\frac{\partial^2 T_e}{\partial x^2}+\frac{\partial^2 T_e}{\partial y^2}=\frac{h_{res}}{b_e k_e}(T_e-T_s)+\frac{h_{resc}}{b_e k_e}(T_e-T_s)+\frac{h_{ega}}{b_e k_e}(T_e-T_{ga})+\frac{h_{egc}}{b_e k_e}(T_e-T_{gc})+\frac{q_E}{b_e k_e} \tag{12}$$

b.c. 1.: at x=0 and x=L, all y; $\dfrac{\partial T_e}{\partial x}=0$

b.c. 2.: at all x, y=0 and y=W; $\dfrac{\partial T_e}{\partial y}=0$

The left-hand terms are conductional heat transfers. The right-hand terms are radiational and convectional heat transfers. The heat of electrochemical reaction, q_E [J/cm^2], is obtained as follows [Nam et al., 1992].

$$q_E=i\cdot\left(-\frac{\Delta H_E}{2F}+V\right) \tag{13}$$

where, ΔH_E [J/mol] is the enthalpy change by the electrochemical reaction [Smith and van Ness, 1987].

$$\Delta H_E=-57{,}018-2.738T+(0.474\times10^{-3})T^2+(2.637\times10^{-6})T^3 \tag{14}$$

3. Current Density and Cell Voltage

Reaction rates of anode and cathode gases and distributions of current density are related to each other in the fuel cell reactions. Detailed models of electrodes, such as the thin film model [Yuh and Selman, 1984] and the agglomerate model [Kunz and Murphy, 1988; Bosio et al., 1999], have been studied. The inclusion of such a micro-model in the macroscopic model has also been tried by Lee et al. [2003]. Selman [1988] has experimentally investigated the detail electrode reaction characteristics involving the gas-phase transport effect. The macroscopic model has been used in this research.

As mentioned above, the current density affected by cell temperatures and also by partial pressures of reactants can be calculated with the other relevant equations. The relationship between current density (i) and cell voltage (V) is written as follows [Appleby and Foulkes, 1989].

$$V=(V_{cN}-V_{aN})-iZ \tag{15}$$

Here, the equilibrium potentials of anode and cathode, V_{aN} and V_{cN}, are derived from the Nernst equation [Appleby and Foulkes, 1989].

$$V_{aN}=V_a^o+\frac{RT}{2F}\ln\left(\frac{X_{aC}X_W}{X_H}\right) \tag{16}$$

$$V_{cN}=V_c^o+\frac{RT}{2F}\ln(X_{cC}X_O^{1/2}) \tag{17}$$

where V_a^o and V_c^o are standard potentials, and X's are compositions of each gas.

The effective cell resistance, Z in Eq. (15), is expressed as follows.

$$Z=R_{ohm}+\frac{\eta_a}{i}-\frac{\eta_c}{i} \tag{18}$$

Anodic and cathodic overpotentials, η_a and η_c in Eq. (18), are obtained by multiplying current density (i) with polarization resistances (Z_a and Z_c).

$$\eta_a=i_aZ_a=iZ_a \tag{19}$$

$$\eta_c=i_cZ_c=-iZ_c \tag{20}$$

In order to quantify the polarizations at the anode and the cathode, Selman [1984] reported:

$$Z_a=2\times0.4567\times10^{-7}(p_H)^{-1.801}(p_{CO})^{1.533}(p_C)^{-1.480}\exp\left(\frac{13{,}140}{T}\right) \tag{21}$$

$$Z_a=7.504\times10^{-6}(p_O)^{-0.43}(p_C)^{-0.09}\exp\left(\frac{9{,}361}{T}\right) \tag{22}$$

The ohmic cell resistance, R_{ohm} in Eq. (18), is evaluated as a function of temperature [Wolf and Wilemski, 1983]. Substituting V_{cN}, V_{aN}, R_{ohm}, η_a and η_c into Eq. (15), the following equation is obtained. The local current density can be calculated with Eq. (23) from the cell voltage and the gas compositions.

$$V=(V_a^o-V_c^o)+\frac{RT}{2F}\ln\left(\frac{X_{cC}X_O^{1/2}X_H}{X_WX_{aC}}\right)-iZ \tag{23}$$

4. Analytical Methods of Calculations

In the mathematical analysis, nine parameters such as cell voltage (V), current density (i), gas compositions (x_i's), temperatures of electrode-electrolyte plate, anode and cathode electrode, and the upper and lower separate plates (T), should be set. However, the number of equations applied to MCFC system is eight; these are Eqs. (6), (7), (8), (9), (12) and (23). Therefore, the degree of freedom in the system is one. In other words, modeling of the MCFC unit cell can be obtained after fixing one parameter value.

One parameter to be fixed can be either cell voltage or current density. In this research, the calculation with a fixed value of cell voltage is named method A and that with a fixed value of current density is named method B. The cell voltage in method A and the current density in method B are assumed distributed uniformly through the whole fuel cell.

The calculation procedures by method A are as follows. First, the current density is supposed as a certain value, such as 150 mA/cm^2. Then the conversion of gases by water-gas shift reaction is calculated and substituted to Eq. (4) to obtain the new gas compositions. These parameters are used in calculating the anode and the cathode ohmic resistances. Finally, a new current density is gained by solving Eq. (23), i.e., the relationship between current density and cell voltage. This procedure is repeated until a new value of current density matches with the previous value within an error range. Then distributions of current density, temperature, and gas compositions are calculated. Calculations by method B are done in a similar way.

Dimensions, flow rates, and gas compositions of the unit MCFC used in the modeling are in Tables 1 and 2.

Table 1. Dimensions of the molten carbonate fuel cell used in the mathematical modeling

Length	(L)	:	10 cm
Width	(W)	:	10 cm
Thickness		:	
Separator	(b_s)	:	0.2 cm
Gas channel	(b_g)	:	0.2 cm
Anode electrode	(b_{ea})	:	0.07 cm
Electrolyte plate	(b_{em})	:	0.1 cm
Cathode electrode	(b_{ec})	:	0.06 cm

Table 2. Flow rates and compositions of the anode gas and the cathode gas at the entrance

	Flow rate (mol/hr)	Compositions	
Anode gas	0.875	H_2	0.68
		CO_2	0.08
		CO	0.12
		H_2O	0.12
Cathode gas	1.050	O_2	0.33
		CO_2	0.67

RESULTS AND DISCUSSIONS

In this study, numerical analyses of the MCFC unit cell were performed at a constant cell voltage and at a constant current density. The temperatures of gases, electrode, electrode-electrolyte plate, and the upper and lower separators, gas compositions, conversions of gases, and cell performances calculated with a fixed value of cell voltage were compared with those calculated with a fixed value of current density.

1. Modeling Calculations

To show that the mathematical modeling is done successfully, calculation results by method A are checked first. By method A, distributions of current density were obtained after the cell voltage was fixed as 0.93 V. Fig. 2 is the contour and the 3-dimensional graphs of the current density. The average value is 94.4 mA/cm^2. However, the value of current density at the gas entrance is about 216 mA/cm^2. It is much higher than the average value. This is because the electro-chemical reaction occurs vigorously at the gas entrance due to the great mole fraction of hydrogen (H_2). The value of the current density decreases along the direction of gas flow and that at the gas outlet becomes 36 mA/cm^2 which is one-fifth of the value at the gas inlet. The current density does not distribute evenly through the cell.

Effects of the water gas shift reaction are in Fig. 3. Curves in the graph are conversions of hydrogen only by the water-gas shift reaction along the direction of gas flow calculated at the constant cell voltages such as 0.9, 0.93, 0.99, and 1.05 V, respectively. Here, the conversion, x_S, is the fraction of hydrogen generated or consumed by the shift reaction at an arbitrary point in the cell. It has a negative value when hydrogen is generated.

Following the equilibrium equation of shift reaction, Eq. (4), the forward reaction produces hydrogen and carbon dioxide and the backward reaction produces water and carbon monoxide. The conversion of hydrogen at the inlet of anode gas in Fig. 3 is 0.03. It means hydrogen is consumed by the water-gas shift reaction as it enters the cell. Additionally, the shift reaction in Eq. (3) progresses in reverse to reach an equilibrium state.

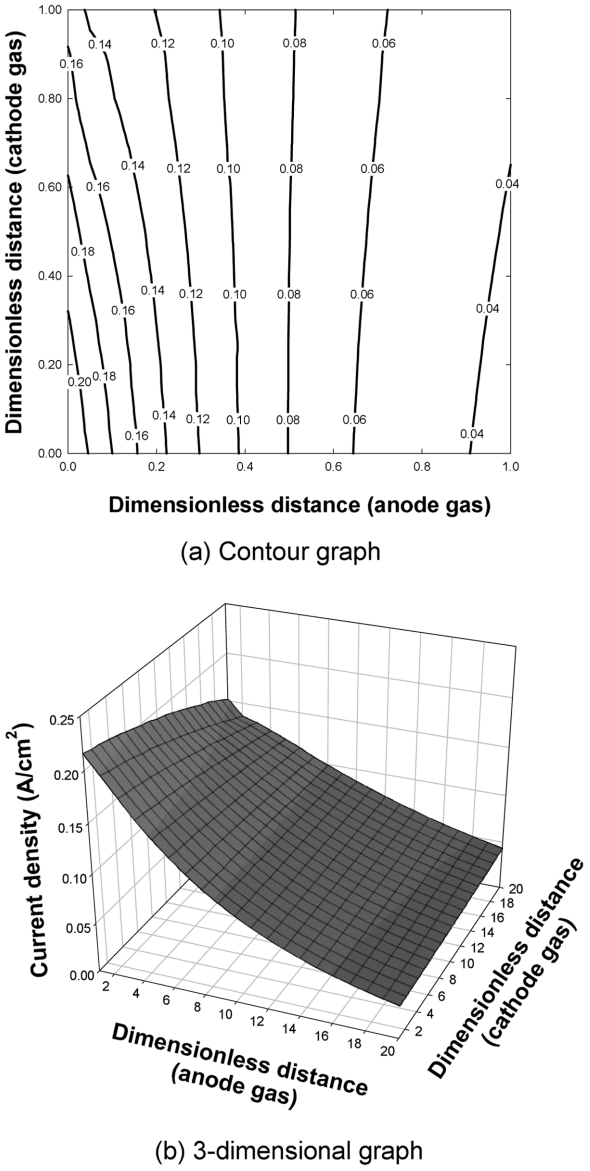

Fig. 2. The current density distributions of the unit cell calculated at a constant cell voltage (0.93 V).

The consumption of hydrogen by the water-gas shift reaction decreases rapidly along the direction of gas flow, and hydrogen is finally generated near the exit. The value of hydrogen conversion by the water-gas shift reaction in Eq. (3) changes from a positive value to a negative one.

The high current density means the electrochemical reaction progresses actively and hydrogen is consumed rapidly. Fig. 4 shows the conversion of hydrogen only by the electrochemical reaction along the direction of gas flow at different average cell voltages. The concentration of hydrogen is high near the gas entrance. Thus, much hydrogen is consumed by the electrochemical reaction and, as a result, the value of current density is high. On the other hand,

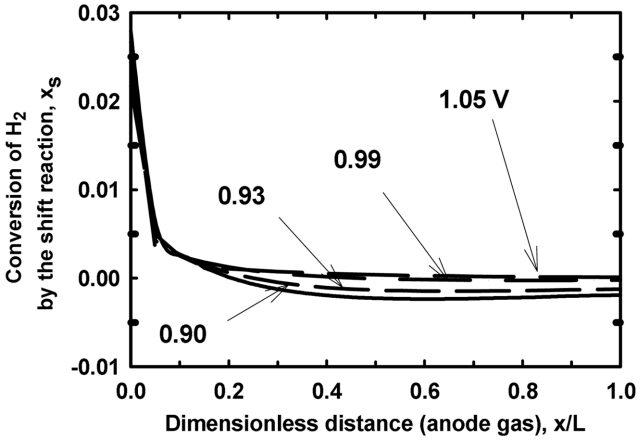

Fig. 3. The conversion of hydrogen only by the water-gas shift reaction along the direction of the anode gas flow at different cell voltages.

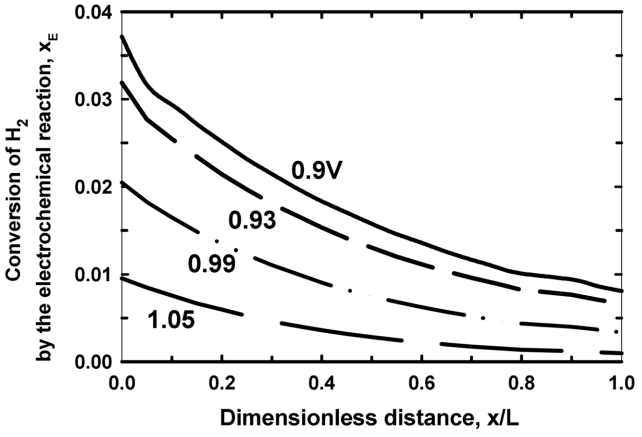

Fig. 4. The conversion of hydrogen only by the electrochemical reaction along the direction of the anode gas flow at different cell voltages.

along the direction of gas flow, the conversion of hydrogen decreases and the current density becomes lower. As expected, the hydrogen conversions by the electrochemical reaction are higher at the lower cell voltages.

2. Comparisons of Temperature Profiles

As mentioned above, the degree of freedom is one in the modeling calculation of a fuel cell. It means that one parameter value should be set to specify the fuel cell system.

Fig. 5 shows the temperature profiles of the electrode-electrolyte plate calculated (a) by the method A--at a constant cell voltage of 0.95 V, and (b) by the method B--at a constant current density of 150 mA/cm^2, respectively. The temperature distributions, calculated by method A with a constant cell voltage, range between 920 K and 924.2 K. On the other hand, the temperature distributions, calculated by method B with a constant current density, range between 920 K and 927.8 K. The calculations done after fixing the value of current density gave a sharper temperature gradient especially at the gas exits.

Distributions of temperature of the electrode-electrolyte plate are influenced by the heat of electrochemical reaction, by the heat of

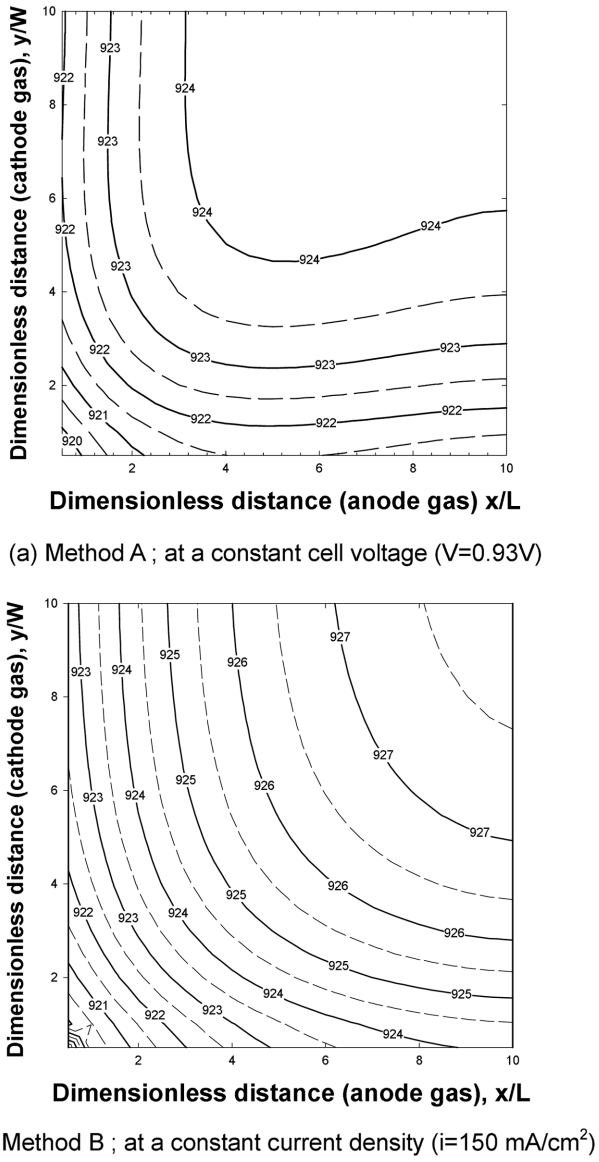

Fig. 5. Contour graphs of the temperature distribution of the electrode-electrolyte plate calculated by two different methods: (method A) at a constant cell voltage (V=0.93 V); (method B) at a constant current density (i=150 mA/cm^2).

water-gas shift reaction, and by the flows of anode and cathode gases. The shift reaction consumes a considerable amount of hydrogen around the inlet of anode gas. So, under the conditions of this research, the heat of water-gas shift reaction is −150.1 J/cm^2 around the inlet of anode gas, which is a negative value. This heat of water-gas shift reaction increases gradually along the gas flow. After the center of the fuel cell, the biggest heat of the water-gas shift reaction becomes 8.2 J/cm^2. Therefore, the fraction of hydrogen in the anode gas affects the temperature distributions. Cathode and anode gases also affect the temperature distributions by convectional heat loss. Hence the temperature profile changes along the direction of anode gas flow and also along the direction of cathode gas flow.

Fig. 6 is the temperature distributions of the upper separator calculated (a) by the method A and (b) by the method B, respectively. The temperature ranges between 917 K and 923.4 K. Differently

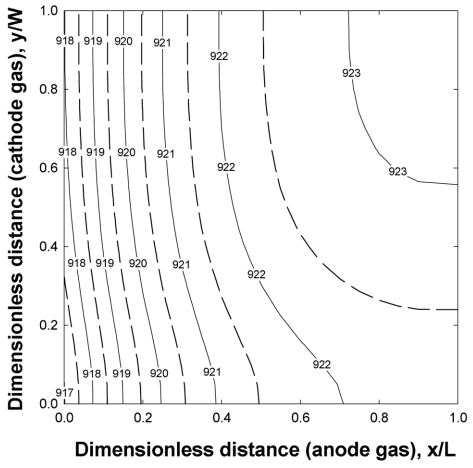

(a) Method A ; calculated at a constant cell voltage (V=0.93V)

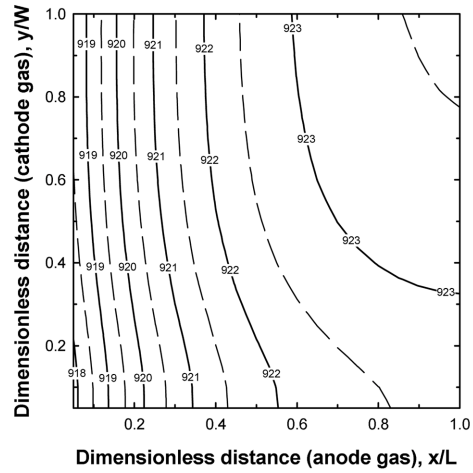

(b) Method B ; calculated at a constant current density (i=150 mA/cm^2)

Fig. 6. Contour graphs of the temperature distribution of the upper separator calculated by two different methods: (method A) at a constant cell voltage (V=0.93 V); (method B) at a constant current density (i=150 mA/cm^2).

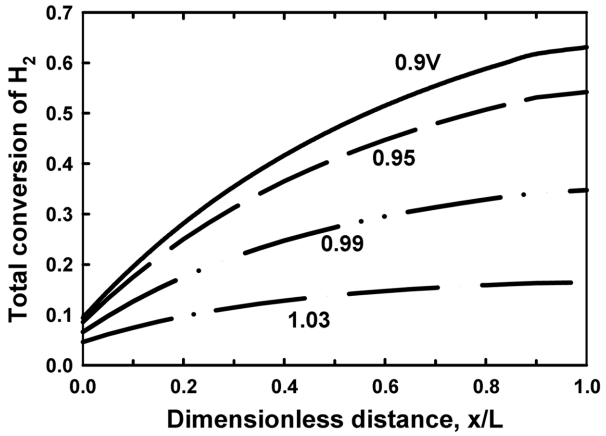

(a) Method A; at a constant cell voltage

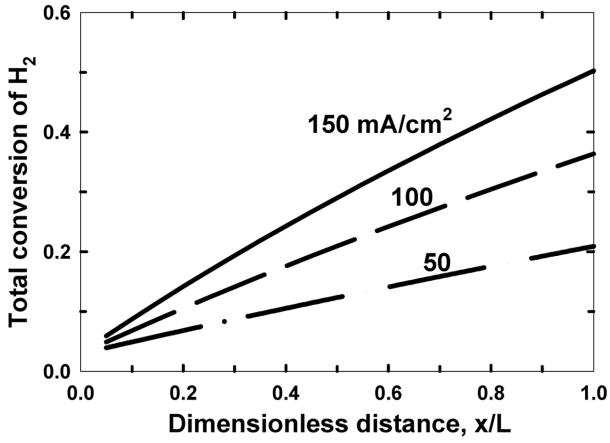

(b) Method B; at a constant current density

Fig. 7. The total conversion of hydrogen along the direction of anode gas flow calculated by two different methods A and B. (a) at different cell voltages; (b) at different average current densities.

from the temperature distributions of the electrode-electrolyte plate, the shapes of temperature contour lines of the upper separator calculated by methods A and B are fairly similar. Because the upper separator is contacting with the anode gas, its temperature increases along the anode gas flow. The temperature gradient at the gas inlet is large due to the high fraction of H_2 in the anode gas and the big cell resistance.

3. Comparisons of Hydrogen Conversions

The conversions of hydrogen in the anode gas calculated by the two methods have been studied. Fig. 7 shows changes of the total conversion of hydrogen along the direction of anode gas flow. Fig. 7(a) is the total conversion of hydrogen calculated at fixed cell voltages of 0.9, 0.95, 0.98 and 1.05 V and Fig. 7(b) is that calculated at fixed current densities of 50, 100, 150 and 200 mA/cm^2. Here the total conversion of hydrogen is defined as the fraction of hydrogen consumed or generated by both the electrochemical reaction and the shift reaction based on the initial amount of hydrogen at the entrance.

Because the current density has been fixed everywhere in the fuel cell in the case of method B, the amount of converted hydrogen is constant everywhere in the cell. So the total amount of reacted hydrogen increases linearly as in Fig. 7(b). The slopes of the conversion line decrease a little bit toward the exit. This is because the shift reaction in Eq. (3) proceeds forward and hydrogen is generated. However, in Fig. 7(a), the total conversion of hydrogen increases and reaches a limit value as the conversion of hydrogen decreases along the anode gas flow. This is relevant to the distributions of the current density. The value of the current density is high around the gas inlet, but it is getting lower along the gas flow. Near the gas outlet, the value of the total conversion of hydrogen changes little as the current density does.

The final total conversions of hydrogen at the exit (x=L), based on the initial amount of hydrogen at the entrance are in Figs. 8(a) and (b). Fig. 8(a) is the results calculated at constant cell voltages of 0.90, 0.93, 0.95 and 1.03 V by the method A. As the value of fixed cell voltage increases, the final total conversion of hydrogen decreases. This is why the value of the current density through the electrode becomes smaller.

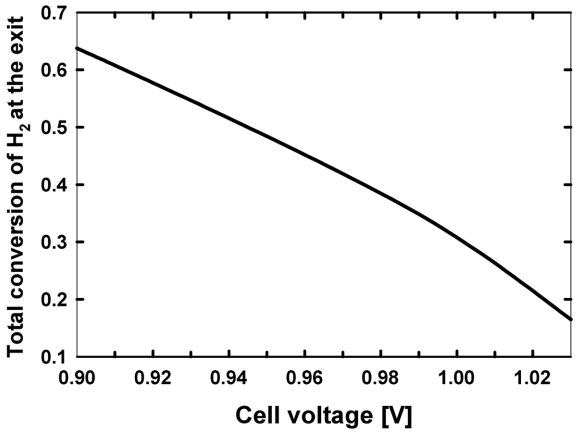

(a) Method A; calculated at fixed values of cell voltage

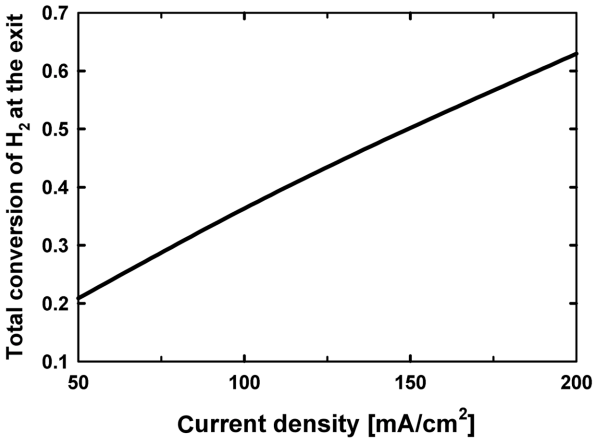

(b) Method B; calculated at fixed values of current density

Fig. 8. The final total conversions of hydrogen at the exit in the anode gas, calculated by two different methods A and B. (a) At different fixed values of cell voltage, (b) At different fixed values of average current density.

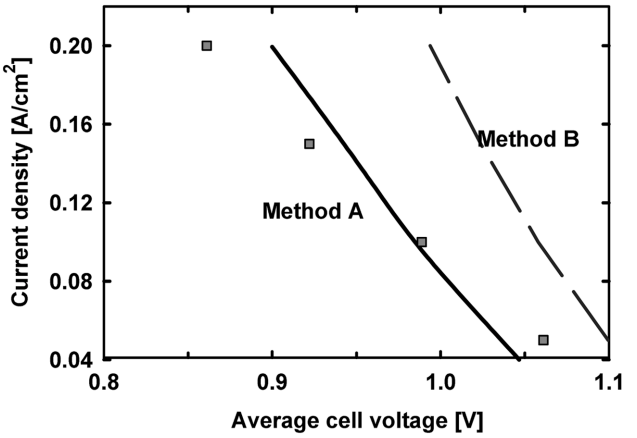

Fig. 9. Comparison of the calculation results of I-V curves with the experimental data [Ahn et al., 1995]. Method A: calculations at fixed values of cell voltage, Method B: calculations at fixed values of current density.

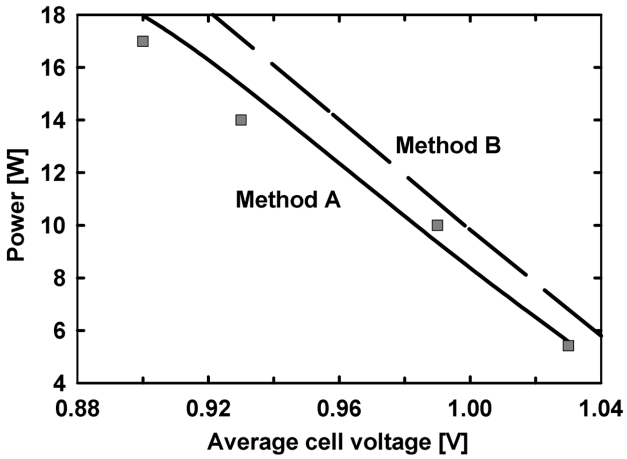

Fig. 10. Comparison of the calculation results of power curves with the experimental data [Ahn et al., 1995].

Fig. 8(b) is the final total conversion of hydrogen at the exit, calculated at constant current densities of 50, 100, 150, 200 mA/cm^2, by method B. On the contrary to the results obtained by calculating at a constant cell voltage, the final total conversion of hydrogen increases as the current density increases. This is because increasing the current density means consuming more hydrogen by the electrochemical reaction when the amount of entering anode gas is constant.

At a small current density such as 50 mA/cm^2, even though the consumed hydrogen by the electrochemical reaction is very small, hydrogen is also consumed by the shift reaction through the whole cell. However, as the current density increases, the amount of carbon monoxide and water, shifted to hydrogen by the reaction in Eq. (3), increases. In another words, the generation of hydrogen by the shift reaction increases. Hence the slope of hydrogen consumption curve decreases a little bit at high current densities.

The decreasing slope of the curve in Fig. 8(a) compared to the constant slope of the curve in Fig. 8(b) shows a clear difference between methods A and B.

4. Comparisons of Cell Performances

Fig. 9 shows changes of current density with the cell voltages calculated by method A and method B. Again, method A is the calculation done at a constant current density and method B at a constant cell voltage. In method A, the average current densities are obtained from the distributions of the current density. In method B, the average cell voltages are calculated from the distributions of the cell voltages. For a cell voltage of 0.95 V, the average current density by method A (calculation at a constant cell voltage) is 0.14 mA/cm^2. This value is much smaller than the calculated current density by method B (calculation at a constant cell voltage). Since the current density distributes through the fuel cell, the local current density changes considerably. Although the current density is very high near the gas entrance, the value gets smaller along the gas flow direction. For this reason, the average current density is very small. As in Fig. 9, the calculation results by method A fit better to the experimental I-V data.

Calculated values of power by methods A and B are compared with experimental data in Fig. 10. Cell performances are obtained by multiplying voltage, current density, and area. Cell performances calculated at a constant cell voltage by method A appeared smaller

compared to those done at a constant current density by method B. This is because of the non-uniform current density distribution. As in Fig. 9, the calculation results by method A fit better to the experimental data than those by method B.

Using the constant value of current density in the calculation by method B is the same as assuming a uniform rate of electrochemical reaction at all parts of the cell. In other words, the results by method A are same as those by method B plus the non-uniformity by the non-uniform electrochemical reaction. Hence, it seems that the calculation results by method A could get closer to the experimental results than those by method B. From the above results, it might be concluded that method A, i.e. the calculation done after fixing a cell voltage, is a better method for the simulation of MCFC.

CONCLUSIONS

A numerical model has been developed to simulate the performance of a unit MCFC. One parameter should be fixed in the process of obtaining results. With one fixed value of cell voltage (method A), distributions of current density and temperature, conversion of hydrogen, and cell performance were obtained. They were also obtained with one fixed value of current density (method B).

By method A, where the cell voltage is fixed, the current density is high near the entrance and it gets low along the direction of gas flow. Hydrogen is consumed near the gas entrance and generated near the gas exit by the water gas shift reaction. Since current density is affected by the fraction of hydrogen, water gas shift reaction contributed to a non-uniform distribution of current density.

For the temperature distributions of the electrode-electrolyte plate obtained by both methods, the calculations done after fixing the value of current density gave a sharper temperature gradient especially at the gas exits. However, the temperature distributions of separators obtained by both methods were similar. Calculations with a fixed value of voltage (method A) gave a slightly lower and more uniform temperature distribution in the separators.

By method B, where the current density is fixed, the amount of reacted hydrogen is constant and the overall hydrogen conversion increases linearly. However, by method A where the voltage is fixed, the conversion of hydrogen near the entrance is high. The non-uniform distribution of current density by method A resulted in lower values of cell performance than those calculated by the method B. Calculated values of cell performance by method A fit better to the experimental data. In conclusion, mathematical modeling done after fixing the value of cell voltage (method A) turns out as a better method than that done after fixing the value of current density (method B).

ACKNOWLEDGMENTS

This work was supported by the New & Renewable Energy Program. The authors acknowledge the financial support from the Ministry of Trade, Industry and Energy through R&D Management Center for Energy and Resources and Korea Electro Power Research Institute (KEPRI).

NOMENCLATURE

b : thickness [m]
C_p : heat capacity
F : Faraday's constant, 26.8 A·hr/mol
G : moles of gas generated and consumed per unit width [mol/cm]
h : heat transfer coefficient [cal/m^2·s·K]
ΔH : enthalpy change by the reaction [J/mol]
i : current density [A/m^2]
k : thermal conductivity [cal/m·s·K]
K : equilibrium constant
L : length of the cell [m]
m : mass of the gas
P : partial pressure [torr]
q : heat of reaction
R : gas constant
n : molar flow rate of gas [mol/s]
R_{ohm} : ohmic cell resistance
T : cell temperature [K]
x, y : x-, y-direction [m]
X : molar fraction
Z : effective cell resistance
V : voltage [V]
W : width of the cell [m]

Greek Letters

η : overpotential [V]
ν : stoichiometric coefficient in the reaction

Superscript

O : standard value

Subscripts

a : anode
b : surroundings
c : cathode
C : CO_2
e : electrode-electrolyte
E : electro-chemical reaction
g : gas
H : hydrogen
i : *i*-th component
N : Nernst equation
O : oxygen
r : radiation
s : shift-reaction
S : separator
W : water

REFERENCES

Ahn, Y. J., Chung, G. Y., Ju, J. B., Nam, S. W., Oh, I. H., Lim, T. H. and Hong, S. A., "Prediction of Temperature Distributions from Mass and Energy Balances and Effects of Operating Parameters in Molten Carbonate Unit Fuel Cell," *HWAHAK KONGHAK*, **32**(6), 830 (1994).

Ahn, Y. J., Chung, G. Y., Ju, J. B., Nam, S. W., Oh, I. H., Lim, T. H. and Hong, S. A., "Numerical Modeling of Effects of Operating Variables of MCFC on the Cell Performance and Comparisons with Experi-

mental Data," *HWAHAK KONGHAK*, **33**(4), 479 (1995).
Appleby, A. J. and Foulkes, F. R., Fuel Cell Hand Book, 539 (1989).
Bosio, B., Costamagna, P. and Parodi, F., "Modeling and Experimentation of Molten Carbonate Fuel Cell Reactors in a Scale-up Process," *Chem. Eng. Sci*., **54**, 2907 (1999).
Cao, G. and Masubuchi, M., "Dynamic Modeling of Molten Carbonate Fuel Cell and its Dynamic Response (Time Response for the Load Change in the Parallel-and Counterflow Types)," *J. Jap. Mech. Eng. Soc.(B)*, **57**, 837 (1991).
Kim, M. H., Chung, G. Y., Nam, S. W., Oh, I. H., Lim, T. H. and Hong, S. A., "The Performances and the Temperature Distributions of the Circular Molten Carbonate Unit Fuel Cell," *J. Energy Engg*., **8**(1), 7 (1999).
Kim, M. H., Park, H. K., Chung, G. Y., Lim, H. C., Nam, S. W., Lim, T. H. and Hong, S. A., "Effects of Water-gas Shift Reaction on Simulated Performance of a Molten Carbonate Fuel Cell," *J. Power Sources*, **103**, 245 (2002).
Kim, T. J., Ahn, Y. J., Ju, J. B., Chung, G. Y., Nam, S. W., Oh, I. H., Lim, T. H. and Hong, S. A., "Effects of the Composition of Nitrogen Gas and the Working Pressure on the Temperature Distributions and Unit Cell Performance of MCFC," *J. Energy Engg*., **4**(3), 354 (1995).
Kobayashi, N., Fujimura, H. and Ohtsuka, K., "Heat and Mass Transfer in a Molten Carbonate Fuel Cell (1st Report, Experimental and Analytical Investigation of Fuel Cell Temperature Distribution)," *J. Jap. Mech. Eng. Soc.(B)*, **54**, 2568 (1988).
Kobayashi, N., Fujimura, H. and Ohtsuka, K., "Heat and Mass Transfer in a Molten Carbonate Fuel Cell (2nd Report, Analysis Investigation of Performance and Temperature Distribution in a Cell Stack)," *J. Jap. Mech. Eng. Soc.(B)*, **57**, 825 (1991).
Koh, J. H., Kang, B. S. and Lim, H. C., "Effect of Various Stack Parameters on Temperature Rise in Molten Carbonate Fuel Cell Stack Operation," *J. Power Sources*, **91**, 161 (2000).
Kunz, H. R. and Murphy, L. A., "Effect of Oxidant Composition on the Performance of Molten Carbonate Fuel Cells," *J. Electrochem. Soc*., **135**(5), 1124 (1988).
Lee, C. G., Kang, B. S., Seo, H. K. and Lim, H. C., "Effect of Gas-phase Transport in Molten Carbonate Fuel Cell," *J. Electroanalytical Chemistry*, **540**, 169 (2003).
Lee, Y. R., Kim, I. G., Chung, G. Y., Lee, C. G., Lim, H. C., Lim, T. H., Nam, S. W. and Hong, S. A., "Studies on the Initial Behaviors of the Molten Carbonate Fuel Cell," *J. Power Sources*, **137**(1), 9 (2004).
Leo, J. M., Bolmen, J. and Mugerwa, M. N., *Fuel Cell Systems*, Plenum Press, 345 (1992).
McCabe, W. L., Smith, J. C. and Harriott, P., *Unit Operations of Chemical Engineering*, McGraw-Hill, New York, 340 (2001).
Nam, S. W., Seo, S. H., Lim, T. H., Oh, I. H., Hong, S. A. and Lim, H. C., "Studies on the Polarization Phenomena in the MCFC," *Hydrogen Energy*, **3**, 55 (1992).
Park, H. K., Lee, Y. R., Kim, M. H., Chung, G. Y., Nam, S. W., Hong, S. A., Lim, T. H. and Lim, H. C., "Studies of the Effects of the Reformer in an Internal-reforming Molten Carbonate Fuel Cell by Mathematical Modeling," *J. Power Sources*, **104**, 140 (2002).
Sampath, V. and Sammels, A. F., "A Performance and Current Distribution Model for Scaled-up Molten Carbonate Fuel Cells," *J. Electrochem. Soc*., **127**, 79 (1980).
Smith, J. M. and van Ness, H. C., *Introduction to Chemical Engineering Thermodynamics*, McGraw-Hill, New York, 698 (1987).
Wolf, T. L. and Wilemski, G., "Molten Carbonate Fuel Cell Performance Model," *J. Electrochem. Soc*., **130**, 48 (1983).
Yuh, C. Y. and Selman, J. R., "Polarization of the Molten Carbonate Fuel Cell Anode and Cathode," *J. Electrochem, Soc*., **131**(9), 2062 (1984).